Resilient Transmission Planning of the Ecuadorian Power System Against Earthquakes

Alex Villamarín-Jácome
Department of Electrical Engineering
Universidad de Chile
Santiago, Chile
avillama@ing.uchile.cl

A. Velásquez-Lozano, M. Saltos-Rodríguez
Department of Electrical and Electronic
Universidad de las Fuerzas Armadas ESPE
Sangolquí, Ecuador
[amvelasquez1, masaltos2]@espe.edu.ec

2022 IEEE Sixth Ecuador Technical Chapters Meeting (ETCM) | 978-1-6654-8744-3/22/$31.00 ©2022 IEEE | DOI: 10.1109/ETCM56276.2022.9935745

***Abstract*—Redundancy and hardening of components in transmission systems are practices to improve system resilience against possible adverse consequences caused by natural hazards. However, power systems planners do not usually recognize the natural hazards, so-called high-impact low-probability (HILP) events, within network investment decisions. The situation is exacerbated by an increase in the frequency and severity of power system blackouts due to HILP-type events. In this context, this paper proposes a planning problem for investment in transmission lines and hardening of substations to improve the resilience of power system considering the outage scenarios originated by earthquakes. The problem is formulated as a mixed-integer linear programming (MILP) approach. Furthermore, a probabilistic methodology is used to simulate the hazard and its impacts on the power system. Our proposal is applied on the Ecuadorian transmission system. The results demonstrate that hardening substations and investment in lines can significantly contribute towards enhancing resilience to high impact exogenous natural hazards.**

***Index Terms*—Resilient transmission planning, hardening substations, resilience, natural hazards, earthquakes.**

NOMENCLATURE

A. Sets

$fr(l)$	Sending or origin bus of transmission line l.
$to(l)$	Receiving or destination bus of transmission line l.
W	Set of contingency indexes.
Ω_n^D	Set of indexes of demands connected to bus n.
Ω^G	Set of generator indexes.
Ω_n^G	Set of indexes of generators connected to bus n.
Ω^L	Set of indexes of existing transmission lines.
Ω^{L+}	Set of indexes of candidate transmission lines.
Ω^N	Set of bus indexes.
Ω^{NH}	Set of indexes candidate hardening buses.

B. Parameters

C_d^{LS}	Load-shedding cost of demand d [$/MWh].
C_i^G	Production cost of generator i [$/MWh].
C_l^L	Investment cost of candidate transmission line l [$].
C_n^N	Investment cost of hardened substation n [$].
$DS_{l,w}^{hdn}$	Damage state of the transmission line l for hardened case under contingency w [%].
$DS_{l,w}^{nrm}$	Damage state of the transmission line l for normal case under contingency w [%].
$DS_{n,w}^{hdn}$	Damage state of the bus n for hardened case under contingency w [%].
$DS_{n,w}^{nrm}$	Damage state of the bus n for normal case under contingency w [%].
M	Big M, sufficiently large positive value.
$\overline{p}_i^G$	Capacity of generator i [MW].
$\overline{p}_l^L$	Capacity of transmission line l [MW].
$\overline{p}_l^{L+}$	Capacity of candidate transmission line l [MW].
p_d^D	Load of demand d [MW].
R_i^U	Power reserve of generator i [MW].
x_l	Reactance of transmission line l [p.u.].
π_w	Probability of contingency w [p.u.].
Π	Investment budget [$].

C. Variables

$A_{d,w}^D$	Derating factor of the demand d under contingency w [%].
$A_{i,w}^G$	Derating factor of the generator i under contingency w [%].
$A_{l,w}^L$	Derating factor of the transmission line l under contingency w [%].
p_d^{LS}	Load shed by demand d [MW].
$p_{i,0}^G$	Power output of generator i in the pre-contingency state [MW].
$p_{i,w}^G$	Power output of generator i under contingency w [MW].
$p_{l,w}^L$	Power flow of transmission line l under contingency w [MW].
$p_{l,w}^{L+}$	Power flow of candidate transmission line l under contingency w [MW].
$\theta_{n,w}$	Phase angle at bus n under contingency w [rad].
v_l	Binary variable that is equal to 1 if candidate transmission line l is built, being 0 otherwise.
z_n	Binary variable that is equal to 1 if candidate substation n is hardened, being 0 otherwise.

This work has been supported by the Scholarship SENESCYT/ARSEQ-BEC-006295-2018.

I. INTRODUCTION

Electric power systems are frequently exposed to catastrophic damage caused by natural hazards, so-called high-impact low-probability (HILP) events. Amongst others, natural hazard such as earthquakes is considered one of the main causes of wide-area power outages worldwide and lead to enormous economic losses and even human fatalities [1]. In Ecuador, for example, the 2016 Pedernales earthquake caused extensive damage to the transmission and distribution systems. The economic losses were estimated at approximately 103 million USD [2]. In addition, the 1987 El Reventador earthquake caused damage to several generation plants and trans-

mission lines. It is estimated that earthquake-incurred losses cost Ecuador 3.8 million USD [2]. Consequently, these facts highlight the need for rethinking current planning practices (i.e., under reliability standards) to allow HILP-type events to be accounted into resilience-driven investment planning. However, designing and building a resilient transmission network can be prohibitively expensive. Therefore, it is fundamental to identify how to cost-effectively allocate limited budget resources to planning a resilient power system against natural hazards.

In this context, there are several studies on resilient transmission planning focuses on the redundancy and hardening of components in transmission networks considering natural hazards or extreme events [3]–[8]. However, few studies address transmission planning considering seismic resilience analysis. Among these, [7] proposes a model to optimize the selection of capacity enhancement strategies to increase the resilience of electric power systems to earthquakes. These strategies include investments in additional transmission and generation margin to the system. Similarly, [8] presents a resilient-constrained generation and transmission expansion planning considering earthquake and flood. This model includes hardening transmission lines, generation units, and series and parallel FACTS devices as resilience sources.

Another way to address enhancing the transmission system resilience against natural hazards in power networks is by hardening substations. Hardening substation by component retrofits is considered, including weight and moments of equipment reductions, use of composite insulator instead of porcelain ones, use of high strength supports, and anchored power equipment [9]. This hardening strategy is key in resilient network planning because substations are the most vulnerable components to major earthquakes [10], whose outages affect every component connected to it (lines, generating units, etc.).

Hence, this paper proposes a planning problem for investment in transmission lines and the hardening of substations to improve the resilience of power system considering the outage scenarios originated by earthquakes. The problem is formulated as a mixed-integer linear programming (MILP) approach. Furthermore, a probabilistic methodology is used to simulate the hazard and its impacts on the power system. This methodology allows to capture a very high level of detail and complexity in the simulation stage, including a comprehensive set of operational constraints and the sequential process of disconnection and reconnection of components, which is key to evaluating the resilience of power systems.

The rest of this paper is organized as follows. Section II describes the methodological framework for optimal resilient planning of power transmission systems against earthquakes. Section III presents the case studies and shows our results. Finally, Section IV summarizes the main conclusions.

II. Methodology

A methodological framework for optimal resilient planning of transmission networks against earthquakes is presented in Fig. 1. This methodology consists of several sequential stages. In the first stage, we use a probabilistic simulation approach to model the seismic hazard and the consequent network outages and their repairs. This stage is run sequentially in a Monte Carlo simulation (MCS) to obtain a detailed simulation of the power system during the earthquake. In the second stage, we propose an optimization problem to identify the optimal resilient network enhancement strategies. This stage includes a set of operational constraints under a number of outage scenarios resulting from the simulation stage. Thereafter, a restoration procedure of the enhanced power network is developed. As a result, the optimal enhancement strategies of resilient transmission network as evaluated through resilience metrics is obtained. The description of each of the stages is detailed below.

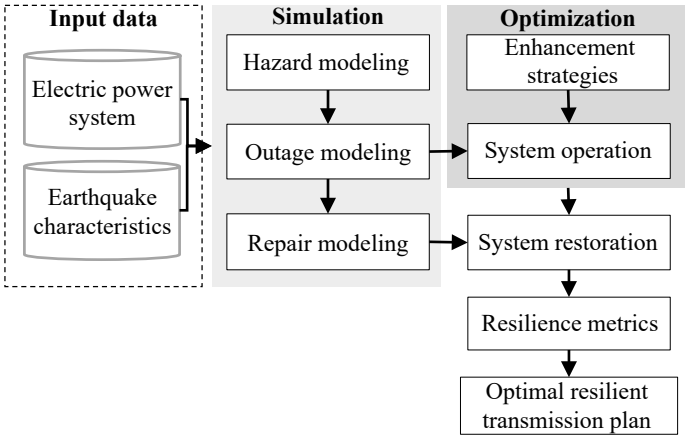

Fig. 1. Methodological framework for optimal resilient planning of transmission systems against earthquakes.

A. Simulation

1) Hazard modeling: In the first step, we calculate the earthquake intensities at the location of each network component. To do so, peak ground acceleration (PGA) proposed in [11] is used as follows (1):

$$PGA_{(r,h,M)} = \frac{e^{6.36+1.76M+0.009h-2.73\log(r+1.58e^{0.608M})}}{980.665} \quad (1)$$

where M is the moment magnitude and h is the focal depth in kilometers. Given the epicenter (ex, ey), then $r = \sqrt{(ex-cx)^2+(ey-cy)^2}$, which is the distance of each component (cx, cy) to the epicenter in kilometers. The results is expressed in [g], the gravity acceleration constant.

2) Outage modeling: In order to generate outage scenarios across the system, we determine the seismic hazard-dependent failure probabilities of vulnerable components. According to the experiences reported in the literature, substations are the most vulnerable components to major earthquakes [10]. Therefore, this work considers only the substation outages triggered by earthquakes, which affect every component connected to it (lines, generating units, etc.).

Then, we determine the probabilities of outages of substations, conditional to earthquake intensities obtained from (1). Indeed, substations may respond differently to earthquakes and, as a result, different damage states with different probabilities are defined based on fragility curves [12]. Specifically,

fragility curves give the probability distribution over two or more damage states as a function of given PGA. We use the approach in [12] with 5 states: (i) none (fully functioning), (ii) slight, (iii) moderate, (iv) extensive, and (v) complete damage. The substation available capacities associated with the (i)–(v) states are 100%, 95%, 60%, 30%, and 0%, respectively. As in dispatch models (needed to determine the system operation and restoration) substations do not explicitly feature a capacity value, a derating factor (associated with damage states) on a substation capacity is applied to equally derates the capacity of all components connected to the substation.

Furthermore, in [12], there are two sets of fragility curves, one to represent substations that have been hardened and another set to represent substations that have not. We use both sets since hardening is a decision variable within the optimal planning problem. This is shown in Fig. 2, where the arrows indicate the shift of the curves due to hardening measures.

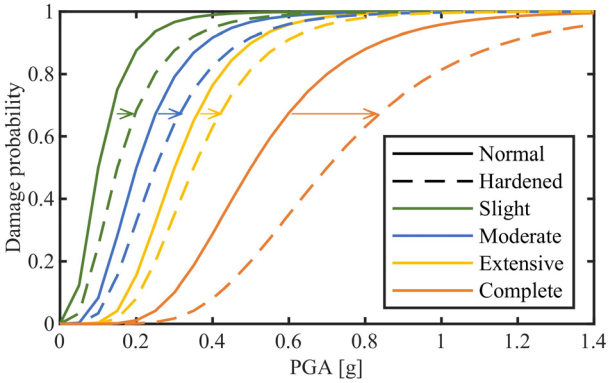

Fig. 2. Substation fragility curves for normal and hardened cases [12].

After we have determined the outage/state probability of every network component, we run MCS to generate various scenarios where network components are outage/derated.

3) Repair modeling: Within this MCS, not only the outages scenarios are generated, but also the repair times of outaged network components, which are determined probabilistically assuming that the reconnection events are exponentially distributed. These repair times are sampled for substations with parameters estimated by Hazus [12].

B. Optimization

The mathematical formulation of the resilient transmission planning problem under the occurrence of multiple outages triggered by earthquakes is presented in this section. The problem can be computed by a mixed-integer linear programming (MILP) model based on the DC power flow. The formulation of the objective function and constraints is presented as follows:

$$\min\ IC + OC \tag{2}$$

$$IC = \sum_{l\in\Omega^{L+}} C_l^L v_l + \sum_{n\in\Omega^{NH}} C_n^N z_n \tag{3}$$

$$OC = \sum_{w\in W}\pi_w \left[\sum_{i\in\Omega^G} C_i^G p_{i,w}^G + \sum_{d\in\Omega^D} C_d^{LS}\left(p_{d,w}^{LS} + p_d^D(1-A_{d,w}^D)\right)\right] \tag{4}$$

s.t.

$$\sum_{l\in\Omega^{L+}} C_l^L v_l + \sum_{n\in\Omega^{NH}} C_n^N z_n \le \Pi \tag{5}$$

$$v_l \in \{0,1\}; \qquad \forall l\in\Omega^{L+} \tag{6}$$

$$z_n \in \{0,1\}; \qquad \forall n\in\Omega^{NH} \tag{7}$$

$$\sum_{i\in\Omega_n^G} p_{i,w}^G + \sum_{l\in(\Omega^L\cup\Omega^{L+})|to(l)=n} p_{l,w}^L - \sum_{l\in(\Omega^L\cup\Omega^{L+})|fr(l)=n} p_{l,w}^L = \sum_{d\in\Omega_n^D}(p_d^D A_{d,w}^D - p_{d,w}^{LS}); \qquad \forall n\in\Omega^N, \forall w\in W \tag{8}$$

$$p_{l,w}^L = \frac{A_{l,w}^L}{x_l}(\theta_{fr(l),w} - \theta_{to(l),w}); \qquad \forall l\in\Omega^L, \forall w\in W\backslash W_0 \tag{9}$$

$$-M(1-v_l) \le p_{l,w}^L - \frac{\theta_{fr(l),w} - \theta_{to(l),w}}{x_l} \le M(1-v_l); \qquad \forall l\in\Omega^{L+}, \forall w\in W \tag{10}$$

$$-\overline{p}_l^L \le p_{l,w}^L \le \overline{p}_l^L; \qquad \forall l\in\Omega^L, \forall w\in W \tag{11}$$

$$-v_l\overline{p}_l^L \le p_{l,w}^L \le v_l\overline{p}_l^L; \qquad \forall l\in\Omega^{L+}, \forall w\in W \tag{12}$$

$$0 \le p_{i,0}^G \le \overline{p}_i^G; \qquad \forall i\in\Omega^G \tag{13}$$

$$0 \le p_{i,w}^G \le (p_{i,0}^G + R_i^U)A_{i,w}^G; \qquad \forall i\in\Omega^G, \forall w\in W \tag{14}$$

$$0 \le p_{d,w}^{LS} \le p_d^D A_{d,w}^D; \qquad \forall d\in\Omega_n^D, \forall w\in W \tag{15}$$

$$A_{d,w}^D = z_n DS_{n,w}^{hdn} + (1-z_n)DS_{n,w}^{nrm}; \qquad \forall n\in\Omega^N, \forall d\in\Omega_n^D, \forall w\in W \tag{16}$$

$$A_{i,w}^G = z_n DS_{n,w}^{hdn} + (1-z_n)DS_{n,w}^{nrm}; \qquad \forall n\in\Omega^N, \forall i\in\Omega_n^G, \forall w\in W \tag{17}$$

$$A_{l,w}^L = z_n DS_{l,w}^{hdn} + (1-z_n)DS_{l,w}^{nrm}; \qquad \forall l\in\Omega^L, \forall w\in W \tag{18}$$

$$DS_{l,w}^{nrm} = \max\left\{DS_{l|fr(l)=n,w}^{nrm}, DS_{l|to(l)=n,w}^{nrm}\right\}; \qquad \forall n\in\Omega^N, \forall l\in\Omega^L, \forall w\in W \tag{19}$$

$$DS_{l,w}^{hdn} = \max\left\{DS_{l|fr(l)=n,w}^{hdn}, DS_{l|to(l)=n,w}^{hdn}\right\}; \qquad \forall n\in\Omega^N, \forall l\in\Omega^L, \forall w\in W \tag{20}$$

The objective function given by (2) corresponds to a global minimization of both investment and system operating costs. Equation (3) includes the investment costs for new lines and hardening substation. Equation (4) indicates the operational costs that includes generation costs and the load-shedding costs plus the term $p_d^D(1-A_{n,w}^D)$, which expresses the derated demand obtained from substation's damage. Constraint (5) denotes the investment budget. Constraints (6) and (7) model the binary nature of investment variables of the candidate lines and candidate substations, respectively. Constraints (8) represent the nodal power balance equations. Constraint (9) and (10) express line flows in terms of nodal phase angles for existing and candidate lines, respectively. Constraints (11) and (12) represent the maximum transfer capacity for existing transmission lines and candidate transmission lines, respectively. Constraint (13) represents the power generation that cannot exceed its maximum capacity. Constraint (14) represents the reserve margins determined in normal state $w \in W_0$. Constraint (15) restricts that the load shed at each bus cannot exceed the load demand at that bus. The amount of load shedding in all buses represents the energy not supplied (ENS) in this study. A detailed description of such constraints can be found in [13], [14].

Constraints (16)-(18) correspond to the derating factor for loads, generators and transmission lines, respectively. Constraints (19) and (20) determine the worst damage state of the transmission lines for normal and hardened cases, respectively.

C. System Restoration

We simulate the reconnection of outaged/damaged network components once substations have been repaired. In this stage, components that fulfill their restoration time are available again. Also, we simulate the reconnection of the generators and loads, which are obtained using a post-contingency dispatch model.

D. Resilience metrics

We use different metrics to measure network resilience from different perspectives, including unsupplied demand, operational resilience, and infrastructure resilience. On the one hand, we use the measurement of the expected ENS (EENS) by sampling across the whole set of outages originated by earthquakes. On the other hand, the operational and infrastructure resilience metrics allow quantifying the resilience in each stage of the collapse-recovery process [15]. We use the following indicators for operational resilience: lost generating capacity and lost load. While for infrastructure resilience, we use the following indicators: outaged lines, outaged generators. Furthermore, we identified the recovery time of infrastructure and operational resilience.

III. Case Studies and Results

To demonstrate the applicability of the proposed methodology to the optimal resilient transmission planning against earthquakes, we use two cases. The first case is used to identify resilience-enhancement investment decisions considering different earthquakes assessed individually in the Ecuadorian transmission system. On the other hand, the second case is used to identify resilience-enhancement investment decisions considering an array of multiple earthquakes in the Ecuadorian transmission system.

A. Input data

1) System description: The Ecuadorian transmission system, which is located in the Pacific Ring of Fire (the most seismically active zone in the world), is modeled through transmission networks with different voltage levels (138 kV, 230 kV and 500 kV), representing its infrastructure in 2020 (shown in Fig.3) [2]. For that year, electricity demand was approximately 3955 MW, and generation supply included mainly hydropower plants (62.58%), and thermal power plants (35.13%), with minor participation from biomass power plants (1.69%), wind power plants (0.26%) and solar power plants (0.33%) [16]. The total installed generation capacity was 7274 MW. The transmission network and power plants data, with their real geographical coordinates can be found in [17]. It is important to mention that the model does not consider detailed distribution networks in order to increase the computational efficiency. For planning purposes, we consider the following 76 candidate network enhancements: 38 new lines and 38 hardening substations. While new lines correspond to extra assets that can be added/installed, hardening substations is a decision for strengthening existing infrastructure. The costs of prospective transmission lines and substation hardening are obtained in [2]. Further details of candidates can be found in [17].

2) Seismic event: For the seismic hazard modeling, we use the characteristics of three historical earthquakes that caused extensive damage in Ecuador. These earthquakes are the 2016 Pedernales, the 1987 El Reventador and the 1797 Riobamba. Table I details the coordinates, magnitude and depth of each of the earthquakes according to [18]. For each earthquake, the PGA is determined at the location of each substation as shown in Fig. 3.

We then generate 1000 scenarios to simulate network outages triggered by each earthquake and repair sequences, via MCS. Once the status of the components (outaged/derated) is obtained, we model the system operation during peak demand, since the earthquake occurs to capture the system degradation as well as the system recovery. Our analysis captures key features of a resilient power network.

The outage scenarios are performed in MATLAB® and the optimization problem is solved in FICO® Xpress. The computations are performed on a computer with Intel(R) Xeon(R) CPU E5-2620 with 2.4 GHz and 32 GB of RAM.

TABLE I
Earthquake Data

Event	Location	Coordinates	Magnitude [Mw*]	Depth [km]
I	Pedernales	0°22'N 79°56'O	7.8	20
II	Riobamba	1°36'S 78°36'O	8.3	15
III	El Reventador	0°05'N 77°22'O	6.9	15

*Moment magnitude scale.

B. Results for individual earthquakes

Table II shows the EENS results for the base case (transmission network without enhancement) compared with the investment case, which considers the network-enhancement investments. In the investment case, we also present the number of hardened substations and new lines installed, and the total investment cost of network enhancements. Note that these results are for each seismic event described above (see Table I).

TABLE II
Investment Results for Individual Earthquakes

Event	*Base case*	*Investment case*			
	EENS [MWh]	EENS [MWh]	New lines	Hardened substation	Total IC [MMUSD]
I	1513.35	737.32	7	24	149.29
II	17264.56	8866.91	10	23	199.52
III	31527.56	7118.62	9	16	118.78

The results show that for the investment case in the three seismic events, EENS is reduced compared to the base case. For the first event, which corresponds to the 2016 Pedernales earthquake, the result of the planning model is to install 7

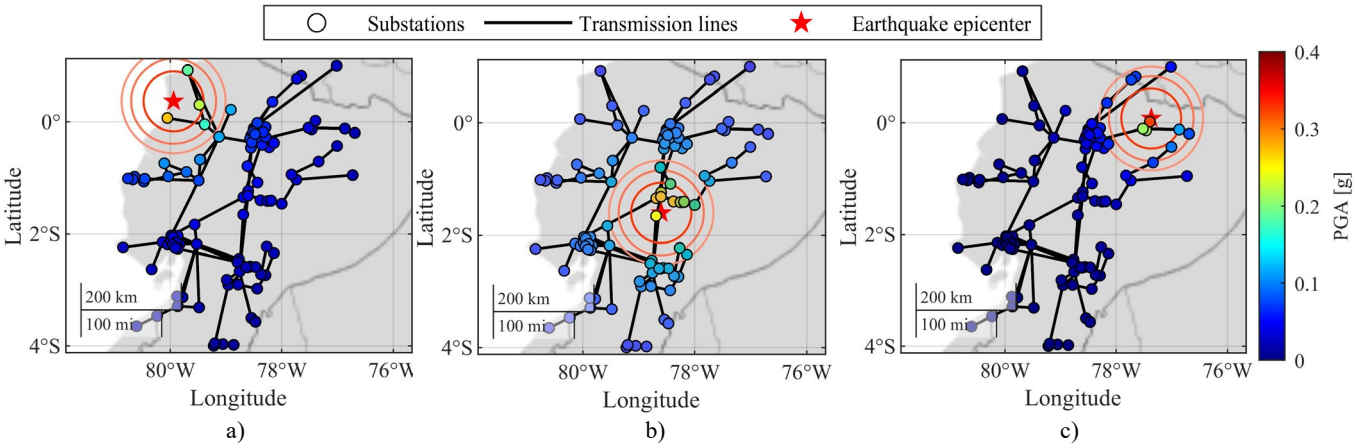

Fig. 3. Ecuadorian transmission system considering the earthquakes: a) 2016 Pedernales, b) 1797 Riobamba and c) 1987 El Reventador.

new lines and the hardening of 24 substations, with this the EENS is reduced by 51.28% (from 1513.35 MWh to 737.32 MWh). For the second event, which corresponds to the 1797 Riobamba earthquake, the result of the investment is to install 10 new lines and the hardening of 23 substations, with this the EENS is reduced by 48.64% (from 17264.56 MWh to 8866.91 MWh). Finally, for the third event, which corresponds to the 1987 El Reventador earthquake, the result of the investment is to install 9 new lines and the hardening of 16 substations, with this the EENS is reduced by 77.42% (from 31527.56 MWh to 7118.62 MWh).

Table III shows the operational and infrastructure resilience metrics obtained for both the base case and the investment case. These metrics allow quantifying the resilience in each stage of the collapse-recovery process. For collapse stage, we use the lost generating capacity and lost load as operational resilience metrics. While for infrastructure resilience, we use the outaged lines and outaged generators. On the other hand, for recovery stage, we compute the recovery time of the energy supplied to the system and recovery of the network infrastructure. The results of the metrics indicate that both operational and infrastructure resilience improve when investment in new lines and hardening of substation are considered. Furthermore, the recovery times are reduced.

TABLE III
RESILIENCE METRICS FOR INDIVIDUAL EARTHQUAKES

Metric	*Base case*			*Investment case*		
	I	**II**	**III**	**I**	**II**	**III**
Lost load [%]	3.99	23.71	22.18	1.95	13.89	7.69
Lost generating capacity [%]	1.01	4.30	4.28	0.66	3.15	2.62
Outaged lines [%]	4.00	16.00	11.00	3.00	13.00	9.00
Outaged generators [%]	0.04	0.81	0.61	0.31	0.31	0.61
Energy recovery [Hours]	168	824	1448	96	336	264
Infrastructure recovery [Hours]	200	304	232	160	288	216

Fig. 4 shows the recovery of the energy supplied post-contingency across 1000 simulations for each restoration stage, ensuring negligible width/error. These results compare system resilience in the base case (blue line) and that of a more resilient system where network enhancements have been implemented by adding new lines and hardening substations (red line). It is interesting to note that these results show that in the three seismic events the inversion solution is capable of reducing the drop in supplied demand and recovering the system in less time than the base case. This is because the hardening of the substation leads to a lower probability of failures and therefore to obtain less outage of the system components. On the other hand, the new lines are capable of strengthening the power network by providing greater redundancy and thus improving the system resilience.

C. Results for multiple earthquakes

Table IV shows the EENS results for the base case (transmission network without enhancement) compared with the investment case, which considers the hardened substations and new lines installed. The results show that the EENS is reduced from 16629.50 MWh to 5821.64 MWh with the investment of 20 new lines and 28 hardened substations. The total investment cost of network enhancements is 299.21 MMUSD. The network enhancements obtained for the Ecuadorian power system is shown in Fig. 5. On the other hand, Table V shows the operational and infrastructure resilience metrics obtained for both the base case and the investment case. In terms of operational and infrastructure resilience, the results show that the investment case caused a decrease in resilience indicators than the base case. These results demonstrate that our methodology is ably to obtain an optimal investment in hardening substations and new lines to enhance the resilience of power systems.

TABLE IV
INVESTMENT RESULTS FOR MULTIPLE EARTHQUAKES

Case	EENS [MWh]	New lines	Hardened substation	Total IC [MMUSD]
Base	16629.50	-	-	-
Investment	5821.64	17	29	299.21

IV. CONCLUSIONS

We propose a planning problem for investment in transmission lines and the hardening of substations to improve the resilience of power system considering the outage scenarios originated by earthquakes. Furthermore, a probabilistic

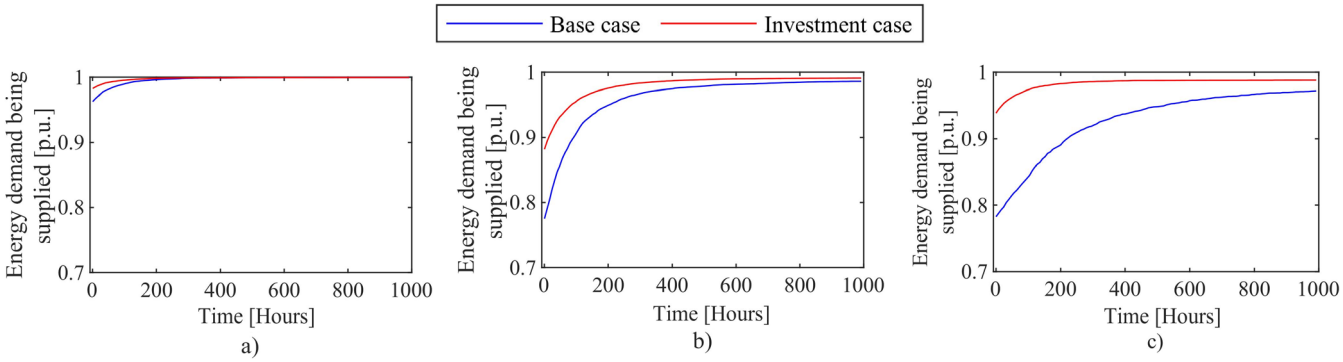

Fig. 4. Recovery process of energy supplied for the base case and investment case considering the earthquakes: a) 2016 Pedernales, b) 1979 Riobamba and c) 1987 El Reventador.

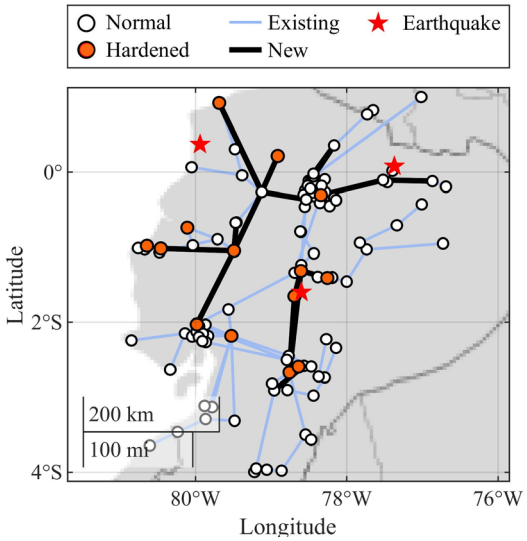

Fig. 5. Results for multiple earthquakes in the Ecuadorian transmission system.

TABLE V
RESILIENCE METRICS FOR MULTIPLE EARTHQUAKES

Metric	***Base case***	***Investment case***
Lost load [%]	16.78	6.82
Lost generating capacity [%]	3.32	2.16
Outaged lines [%]	10	8
Outaged generators [%]	0.47	0.47
Energy recovery [Hours]	888	632
Infrastructure recovery [Hours]	184	152

methodology is used to simulate the seismic hazard and its impacts on the power system. The proposed approach is applied on the Ecuadorian transmission system considering the impacts of a set of the strongest earthquakes recorded in Ecuador.

The results demonstrate that hardening substations and investment in lines can significantly contribute towards enhancing resilience to adverse impacts of large earthquakes. Finally, note that although we assess the proposed modeling framework on earthquakes, this framework can also be applied to other hazards and power systems.

REFERENCES

[1] Y. Wang, C. Chen, J. Wang, and R. Baldick, "Research on resilience of power systems under natural disasters—a review," *IEEE Transactions on Power Systems*, vol. 31, no. 2, pp. 1604–1613, 2016.

[2] "PLAN MAESTRO DE ELECTRICIDAD available: https://www.recursosyenergia.gob.ec/plan-maestro-de-electricidad/," 2022.

[3] A. Bagheri, C. Zhao, F. Qiu, and J. Wang, "Resilient transmission hardening planning in a high renewable penetration era," *IEEE Transactions on Power Systems*, vol. 34, no. 2, pp. 873–882, 2019.

[4] B. J. Pierre, B. Arguello, A. Staid, and R. T. Guttromson, "Investment optimization to improve power system resilience," in *2018 IEEE International Conference on Probabilistic Methods Applied to Power Systems (PMAPS)*, pp. 1–6, 2018.

[5] H. Nagarajan, E. Yamangil, R. Bent, P. Van Hentenryck, and S. Backhaus, "Optimal resilient transmission grid design," in *2016 Power Systems Computation Conference (PSCC)*, pp. 1–7, 2016.

[6] X. Liu, K. Hou, H. Jia, J. Zhao, L. Mili, X. Jin, and D. Wang, "A planning-oriented resilience assessment framework for transmission systems under typhoon disasters," *IEEE Transactions on Smart Grid*, vol. 11, no. 6, pp. 5431–5441, 2020.

[7] N. Romero, L. Nozick, I. Dobson, N. Xu, and D. Jones, "Transmission and generation expansion to mitigate seismic risk," *IEEE Transactions on Power Systems*, vol. 28, no. 4, pp. 3692–3701, 2013.

[8] H. Hamidpour, S. Pirouzi, S. Safaee, M. Norouzi, and M. Lehtonen, "Multi-objective resilient-constrained generation and transmission expansion planning against natural disasters," *International Journal of Electrical Power and Energy Systems*, vol. 132, p. 107193, 2021.

[9] M. Oboudi, M. Mohammadi, D. Trakas, and N. Hatziargyriou, "A systematic method for power system hardening to increase resilience against earthquakes," *IEEE Systems Journal*, vol. 15, no. 4, pp. 4970–4979, 2021.

[10] H. Rudnick, S. Mocarquer, E. Andrade, E. Vuchetich, and P. Miquel, "Disaster management," *IEEE Power and Energy Magazine*, vol. 9, no. 2, pp. 37–45, 2011.

[11] C. Crouse, "Ground-motion attenuation equations for earthquakes on the cascadia subduction zone," *Earthquake spectra*, vol. 7, no. 2, pp. 201–236, 1991.

[12] FEMA, "Hazus - mh mr5: Technical manual," *Federal Emergency Management Agency, Washington, DC*, 2015.

[13] A. Villamarín, R. Haro, M. Aguirre, and D. Ortíz, "Evaluación de resiliencia en el sistema eléctrico ecuatoriano frente a eventos sísmicos," *Revista Técnica" energía"*, vol. 17, no. 2, pp. 18–28, 2021.

[14] M. Saltos-Rodríguez, M. Aguirre-Velasco, A. Velásquez-Lozano, A. Villamarín-Jácome, J. Haro, and D. Ortiz-Villalba, "Resilience assessment in electric power systems against volcanic eruptions: Case on lahars occurrence," in *2021 IEEE Green Technologies Conference (GreenTech)*, pp. 305–311, 2021.

[15] M. Panteli, P. Mancarella, D. N. Trakas, E. Kyriakides, and N. D. Hatziargyriou, "Metrics and quantification of operational and infrastructure resilience in power systems," *IEEE Transactions on Power Systems*, vol. 32, no. 6, pp. 4732–4742, 2017.

[16] "INFORME ANUAL 2020 available: http://www.cenace.gob.ec/informe-anual-2020/," 2022.

[17] Test system data. [Online], Available: https://drive.google.com/drive/folders/1ZYfiS1qGU-fovx7_9CUwox6Ej6gQyR9p?usp=sharing.

[18] "INSTITUO GEOFÍSICO EPN available: https://www.igepn.edu.ec/," May 2022.